A new low-voltage-driven GRIN liquid crystal lens with multiple ring electrodes in unequal widths

Yung-Yuan Kao,[1] Paul C.-P. Chao,[1,*] and Chieh-Wen Hsueh[1]

[1]*Department of Electrical Engineering, National Chiao Tung University, 1001 University Road, Hsinchu 300, Taiwan*
**pchao@mail.nctu.edu.tw*

Abstract: This work is dedicated to design a novel liquid crystal (LC) lens device with multiple ring electrodes in unequal widths, in order to offer tunability on focusing quality and to lower the level of applied voltage. The number and widths of the multiple ring electrodes are pre-designed and optimized to offer the on-line tunability on individual electrode voltages to render a better refraction index distribution for focusing, as compared to the past hole-type LC lenses. The resulted refractive index distribution is expected to offer similar focusing effects based on the theory of the gradient refraction index (GRIN) lens. The transparent electrodes of this new LC lens are placed at the inner surface of the LC cell to minimize the driving voltages, in results, less than 10V, for the same level of focusing power and an easy practical operation. A new fabrication process in the wafer level to bury bus lines is developed for generating smooth electrical fields over the lens aperture. In addition, a dielectric layer is coated between electrodes and the LC layer.

OCIS codes: (230.3720) Liquid-crystal devices; (220.3630) Lenses; (230.2090) Electro-optical devices.

References and links

1. S. Sato, "Liquid-crystal lens-cells with variable focal length," Jpn. J. Appl. Phys. **18**(9), 1679–1684 (1979).
2. T. Nose, and S. Sato, "A liquid crystal microlens obtained with a nonuniform electric field," Liq. Cryst. **5**(5), 1425–1433 (1989).
3. A. Naumov, G. D. Love, M. Yu. Loktev, and F. L. Vladimirov, "Control optimization of spherical modal liquid crystal lenses," Opt. Express **4**(9), 344–352 (1999).
4. B. Wang, M. Ye, M. Honma, T. Nose, and S. Sato, "Liquid crystal lens with spherical electrode," Jpn. J. Appl. Phys. **41**(Part 2, No. 11A), L1232– L1233 (2002).
5. P. J. W. Hands, A. K. Kirby, and G. D. Love, "Adaptive modally addressed liquid crystal lenses," Liquid Crystals VIII, Proc. of SPIE **5518**, Liq. Cryst. VIII, 136–143 (2004).
6. M. Ye, S. Hayasaka, and S. Sato, "Liquid crystal lens array with hexagonal-hole-patterned electrodes," Jpn. J. Appl. Phys. **43**(No. 9A), 6108–6111 (2004).
7. B. Wang, M. Ye, and S. Sato, "Liquid crystal lens with stacked structure of liquid-crystal layers," Opt. Commun. **250**(4-6), 266–273 (2005).
8. M. Ye, and S. Sato, "Optical properties of liquid crystal lens of any size," Jpn. J. Appl. Phys. **41**(Part 2, No. 5B), L571–L573 (2002).
9. M. Ye, B. Wang, and S. Sato, "Liquid-crystal lens with a focal length that is variable in a wide range," Appl. Opt. **43**(35), 6407–6412 (2004).
10. C. W. Chiu, Y. C. Lin, P. C. P. Chao, and A. Y. Fuh, "Achieving high focusing power for a large-aperture liquid crystal lens with novel hole-and-ring electrodes," Opt. Express **16**(23), 19277–19284 (2008).
11. Y. H. Lin, H. Ren, K. H. Fan-Chiang, W. K. Choi, S. Gauza, X. Zhu, and S. T. Wu, "Tunable-Focus Cylindrical Liquid Crystal Lenses," Jpn. J. Appl. Phys. **44**(No. 1A), 243–244 (2005).
12. M. Bin Wang, "Ye, M. Yamaguchi, and S. Sato, "thin liquid crystal with low driving voltages," Jpn. J. Appl. Phys. **48**, 098004 (2009).
13. H. Ren, Y. H. Fan, and S. T. Wu, "Tunable Fresnel lens using nanoscale polymer-dispersed liquid crystals," Appl. Phys. Lett. **83**(8), 1515–1517 (2003).
14. P. Valley, D. L. Mathine, M. R. Dodge, J. Schwiegerling, G. Peyman, and N. Peyghambarian, "Tunable-focus flat liquid-crystal diffractive lens," Opt. Lett. **35**(3), 336–338 (2010).
15. T. C. Kraan, T. van Bommel, and R. A. Hikmet, "Modeling liquid-crystal gradient-index lenses," J. Opt. Soc. Am. A **24**(11), 3467–3477 (2007).

#127370 - $15.00 USD Received 22 Apr 2010; revised 2 Aug 2010; accepted 3 Aug 2010; published 16 Aug 2010

16. M. P. C. M. Krijn, S. T. de Zwart, D. K. G. de Boer, O. H. Willemsen, and M. Sluijter, "2-D/3-D displays based on switchable lenticulars," J. Soc. Inf. Disp. **16**(8), 847–855 (2008).
17. M. Sluijter, A. Herzog, D. K. G. de Boer, M. P. C. M. Krijn, and H. P. Urbach, and H. P. Urbach, "Ray-tracing simulations of liquid-crystal gradient-index lenses for three-dimensional displays," J. Opt. Soc. Am. B **26**(11), 2035–2043 (2009).
18. M. Kurihara, and N. Hashimoto, "Liquid crystal optics for laser beam modulation," Proc. SPIE **6374**, U101–U106 (2006).
19. C.-C. Cheng, C. A. Chang, C.-H. Liu, and J. A. Yeh, "A tunable liquid-crystal microlens with hybrid alignment," 2009 SID International Symposium Digest of Technical Papers, **8**, S365–S369–114 (2006).
20. Y.-Y. Kao, Y.-P. Huang, K.-X. Yang, P. C.-P. Chao, C.-C. Tsai, and C.-N. Mo, ""An auto-stereoscopic 3D display using tunable liquid crystal lens array that mimics effects of GRIN lenticular lens array," 2009 SID International Symposium," Dig. Tech. Pap. **XL**, 111–114 (2009).
21. G. Li, P. Valley, P. Äyräs, D. L. Mathine, S. Honkanen, and N. Peyghambarian, "High-efficiency switchable flat diffractive ophthalmic lens with three-layer electrode pattern and two-layer via structures," Appl. Phys. Lett. **90**(11), 111105 (2007).
22. E. Hecht, *Optics,* (Addision-Wesley, 2002).
23. N. Damean, B. A. Parviz, J. N. Lee, T. Odom, and G. M. Whitesides, "Composite ferromagnetic photoresist for the fabrication of microelectromechanical systems," J. Micromech. Microeng. **15**(1), 29–34 (2005).
24. J. W. Goodman, *Introduction to Fourier Optics* (McGraw-Hill, 1968).
25. N. Fraval, and J. L. B. de la Tocnaye, "Low aberrations symmetrical adaptive modal liquid crystal lens with short focal lengths," Appl. Opt. **49**(15), 2778–2783 (2010).
26. T. Takahashi, M. Ye, and S. Sato, "Wavefront aberrations of a liquid crystal lens with focal length variable from negative to positive values," Jpn. J. Appl. Phys. **46**(No. 5A), 2926–2931 (2007).
27. H. Ren, D. W. Fox, B. Wu, and S. T. Wu, "Liquid crystal lens with large focal length tunability and low operating voltage," Opt. Express **15**(18), 11328–11335 (2007).

1. Introduction

A liquid crystal (LC) lens was first introduced by Sato in 1979 [1]. The lenses shaped like a plano-convex or concave lens with the focal lens varied between f_e and f_o, which are corresponding to effective focal lengths for the extraordinary and ordinary rays. A hole-patterned electrode and with an indium-tin oxide (ITO-) coated counter-electrode were presented later by [2] for generating non-uniform electrical field to generating focusing effects. It is noted that the hole-type LC lens does not offer an exact prefect index distribution (a quadratic-like distribution) for focusing, especially for the case of large aperture. Also, the glass substrate adopted is necessarily thick for a satisfactory index distribution, leading to the requirement of high voltage application. Following [2], there were a number of reported works [2–12] presenting variations of LC lens designs with varied electrode shapes, like circular, cylindrical, and hexagonal-hole-patterned ones. Some others adopted the design principle of Fresnel zone plate [13,14], but rendering less focusing power from higher-order focused lights. Except for those in zone plates, all the studies are devoted for a better index distribution (as close as possible to the GRIN lens [15–20]) and/or decreasing applied voltage level. Some works used high resistance materials to form the electrodes [21], while others used two LC layers for a short focusing length [14].

A new type of the LC lens with multiple circular electrodes in unequal widths and associated new fabrication process is proposed in this study. The unequal-width electrodes are designed to cover the entire aperture for fine-tuning the generated electric field. With the on-line tunability to individual electrode voltages, the designed LC lens is able to achieve a quadratic-like index distribution for better focusing than the conventional hole-type LC lens. Another advantage is the possibility of decreasing driving voltages, since the multiple transparent ring electrodes are placed at the inner surface of the glass substrate, much close to the LC layer than past works. Also, in order to achieve smooth out desired electrical fields with inner electrodes, a thin insulator film is coated between LC and electrode layers to smooth out the desired index distribution. Finally, a new fabrication process is developed to bury the bus lines under the ring electrodes, in order to avoid undesired electric field distortion near the bus lines. This advantage of avoiding distortions were reported in [21] with similar structure but equal electrode widths. Experiments are conducted for performance validation. The resulted data demonstrate well favorable focusing properties offered by the proposed LC GRIN lens in terms of interference pattern, focusing power and tenability on focusing effects.

#127370 - $15.00 USD Received 22 Apr 2010; revised 2 Aug 2010; accepted 3 Aug 2010; published 16 Aug 2010

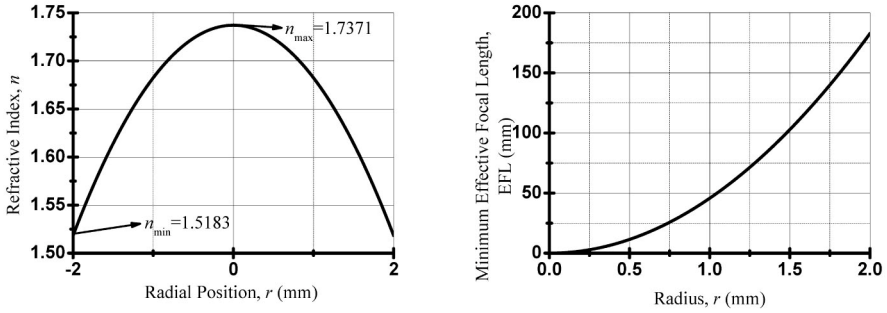

(a) (b)

Fig. 1. (a) The refractive index distribution of a GRIN lens with 2 mm in radius; (b) The relationship between the lens aperture and the minimum effective focal length possible.

2. Design principles

A gradient index (GRIN) lens owns the refractive index distributed in a particular gradient manner along the radial direction of the lens [22]. In this way, it acts like a conventional converging/diverging lens, but does not need to be shaped like one and moving and axial motions to realize focusing and/or zooming. Based on this basic GRIN lens principle, the LC lens proposed in this study is designed to own the index distribution along the radial direction of the LC lens as

$$n_G(r) = n_{G,\max} - \frac{r^2}{2d_G f}, \tag{1}$$

where r and $n_{G,max}$ are the radius of the GRIN lens and the associated maximum refractive index, respectively. In addition, the lens thickness is denoted as d_G, while f is the resulted focal length. The index change along the radial direction of the LC GRIN lens also needs to follow Eq. (1). Based on this equation, with appropriate designs of index distribution d_G, $n_G(r)$ and $n_{G,max}$, a desired focal length of the LC GRIN lens f can be achieved, yielding

$$f = \frac{r^2}{2d_{LC}\left[n_{LC,\max} - n_{LC}(r)\right]}, \tag{2}$$

where the subscript LC denotes liquid crystal. Note from the above equation that the focal length of the LC lens is proportional to the square of r and in an inverse proportion to the lens thickness and the difference between $n_{LC,max}$ and $n_{LC}(r)$. The LC material produced by Merck Inc., E7, is employed in this study to design and realize the LC GRIN lens. To initialize the design process with the aim to maximize the LC lens performance, the achievable lower limit of the focal length f ought to be as small as possible for a wide range of applications, e.g., uses in the camera modules of cell phones. Based on Eq. (2), a small f can be achieved by a large d_{LC} and/or $\left[n_{LC,\max} - n_{LC}(r)\right]$. Since a large d_{LC} eventually requires a high voltage drive for small f 's, $\left[n_{LC,\max} - n_{LC}(r)\right]$ is designed to be maximized at this step with assigning n_e of E7 as $n_{LC,max}$. Also based on the basic principles of LC materials and LC lens operation, $n_{LC}(r)$ is designed to be increased up to n_o at the edge of the lens, $r = R$. The lens aperture can be then determined by

$$R = \sqrt{2d_{LC}f\left[n_{LC,\max} - n_{LC}(R)\right]} = \sqrt{2d_{LC}f\left[n_{LC,\max} - n_{LC,\min}\right]} = \sqrt{2d_{LC}f\left[n_e - n_o\right]}. \tag{3}$$

#127370 - $15.00 USD Received 22 Apr 2010; revised 2 Aug 2010; accepted 3 Aug 2010; published 16 Aug 2010

Abiding by the above design principles, the lens refractive index can be depicted as opposed to the lens radial position, as shown in Fig. 1(a), from $n_{LC,max}$ in the middle until $n_{LC}(r)$ in Eq. (2) reaches the minimum possible index of LC molecules in rotation, which is in fact $n_{min} = n_o$. The lens aperture is then determined by Eq. (3). With a chosen LC material E7, once the minimum effective focal length (EFL) of the LC lens is determined, the lens aperture size is decided, and vice versa. Figure 1(b) depicts this relationship between the designed lens aperture radius and the desired minimum EFL, where a monotonic quadratic-curve-like relationship exists. This means that for a given LC material a lens with ability to focus a close objective is necessarily in a relatively small aperture size. For an exemplary study herein, where a moderate lens aperture is considered for design convenience in a lens module in commercial cell phones, the lens is designated as large as R = 2 mm in radius, while the cell gap of the LC lens chosen as d_{LC} = 50um. In results, the LC lens could reach a focal length f of 182.8mm.

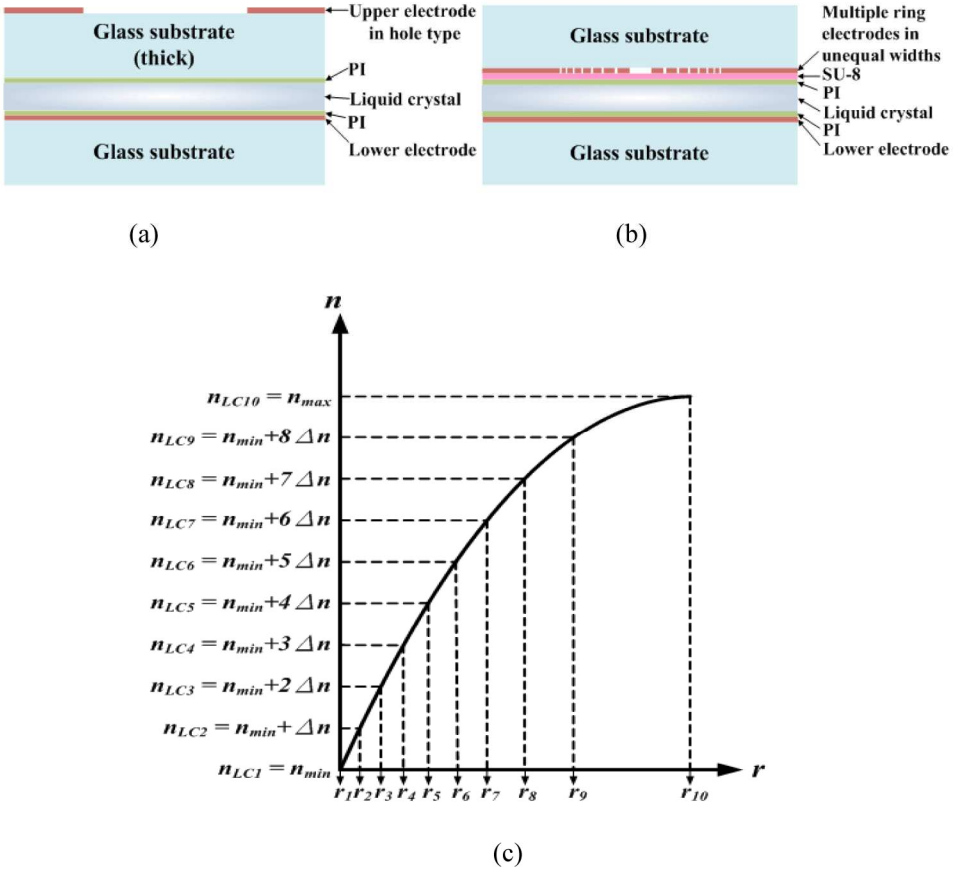

Fig. 2. (a) The structure for the conventional hole-type LC lens; (b) The proposed LC GRIN lens with multiple ring electrodes in unequal widths; (c) The chart for width design of ring electrodes.

#127370 - $15.00 USD Received 22 Apr 2010; revised 2 Aug 2010; accepted 3 Aug 2010; published 16 Aug 2010

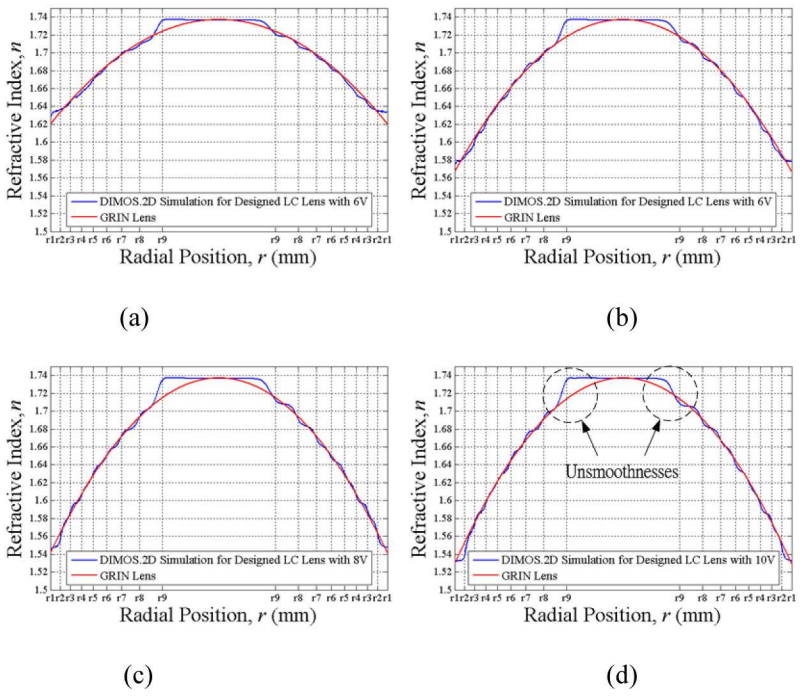

Fig. 3. The simulated refractive index distributions of the proposed LC lens with multiple electrodes in unequal widths and the maximum (for the outmost ring) driving voltages as (a) 4V, (b) 6V, (c) 8V, and (d) 10V.

Aimed for a satisfactory focusing effect, the drive voltages applied to the LC lenses in past studies, like [1], are unavoidably high to achieve a smooth and parabolic-like refraction index distribution across the LC layer. This is due to that fact that the hole-type ITO electrode needs a relatively thick glass layer between the ITO electrode and LC layer, as shown in Fig. 2(a), to generate a smooth parabolic distribution of refraction index, like a perfect GRIN lens with a quadratic index distribution. Due to this thick glass layer, the applied voltage has to be high enough to result in a strong electric field across the LC layer, particularly in the central region of the LC lens. To decrease the drive voltage level for a much easier practical operation and also on-line tenability on focusing quality, a new lens structure as shown in Fig. 2(b) is proposed with multiple ITO ring electrodes coated at the inner surface of the top glass. These electrode rings are expected to bear different pre-designed applied voltages for generating a close-to-quadratic refraction index distribution over the LC layer that mimics a GRIN lens. The design concept herein is close to a Fresnel lens [22] (not a Fresnel zone plate lens). The two polyimide (PI) layers are used for realizing LC alignments. Without a thick glass layer between the upper electrode and LC layer, the proposed LC lens needs much less applied voltage levels to achieve the same focus length as the hole-type lens.

The proposed LC lens structure shown in Fig. 2(b), however, faces a challenge that was already solved in the past works [2–11] by a thick glass layer as shown in Fig. 2(a). The challenge is how to smooth the resulted index distribution in practice with more than one electrode (it was solved by a thick glass and a hole-type electrode by past studies) and also make the distribution close to a quadratic function. To tackle the challenge, two measures are adopted. The first one is to design the individual widths of finite number of ring electrodes as proportional to the gradients of the desired index versus the lens radial position. The second one is to coat a photoresist SU8 layer as a high-dielectric insulator between the top ITO electrode rings and the LC layer to smooth the electric field distribution and then resulted in desired index distribution for focusing. Note that the optical transmittance through the coated SU8 is about 85% at visible spectrum and its dielectric constant is as high as 3 [23].

#127370 - $15.00 USD Received 22 Apr 2010; revised 2 Aug 2010; accepted 3 Aug 2010; published 16 Aug 2010

Table 1. Applied individual electrode voltages

	Applied Voltages (volts)								EFL (mm)	RMSE errors (λ)
Electrode No.	1	2	3	4	5	6	7	8		
	2	2.35	2.7	2.9	3.35	3.6	3.9	4	632.11	0.19
	2.1	2.5	2.9	3.2	3.8	4.2	4.7	5	451.51	0.34
	2.9	3.45	3.95	4.35	4.95	5.5	5.9	6	351.17	0.34
	2.9	3.5	4.05	4.45	5.1	5.8	6.55	7	263.38	0.31
	2.9	3.5	4.15	4.5	5.3	6	6.7	8	225.75	0.35
	2.95	3.55	4.2	4.6	5.5	6.25	7.25	9	210.70	0.5
	2.95	3.55	4.2	4.8	5.7	6.5	7.8	10	182.8	0.58

Efforts are next paid to determine the widths of ring electrodes, which is started with designing the electrode widths as proportional to gradients of the desired index, as illustrated by the chart in Fig. 2(c). In this figure, a half profile of the refraction index distribution for a GRIN lens shown in Fig. 1(a) is considered to determine electrode widths. The total index span from n_o (n_{min}) to n_e (n_{max}) along the ordinate in Fig. 2(c) is first divided to N equal segments. The resulted single index increment is

$$\Delta n = \frac{n_{\max} - n_{\min}}{N} = \frac{n_e - n_o}{N}. \tag{4}$$

The lens radii r_i's as denoted on the abscissa of Fig. 2(c) are designated as the edges of ring electrodes, since they are corresponding to those segmenting indexes $n_{LC,i}$'s on the ordinate. The electrode rings are designed to be placed between r_i's with widths limited by these adjacent r_i's. In this way, each electrode is responsible for the same index increment Δn. The applied voltage differences between adjacent electrodes are also responsible for the same index increment. Thus, it is highly plausible that the required set of applied electrode voltages to achieve a GRIN-lens-like distribution in Fig. 2(c) is linearly distributed over a finite range, making it much easier to realize an external drive circuit. It is also pertinent to note herein that the designed electrode widths between r_i's as shown in Fig. 2(c) are wider in the central region of the lens than at the edge. This is due to the fact that the LC molecules in the central region need much less rotations (low electrical field required) to provide required index change from n_e.

#127370 - $15.00 USD Received 22 Apr 2010; revised 2 Aug 2010; accepted 3 Aug 2010; published 16 Aug 2010

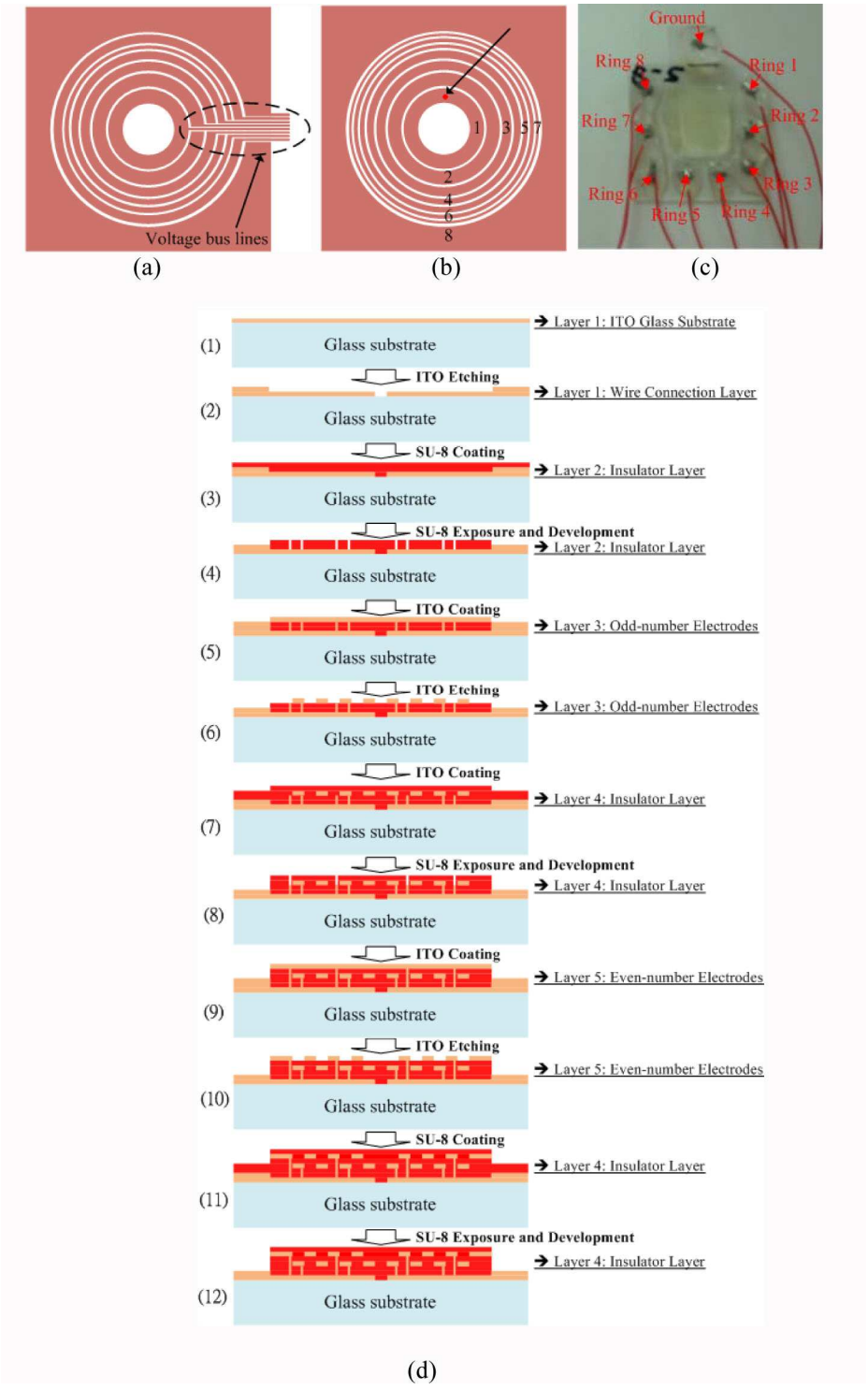

Fig. 4. (a) The electrode pattern with all electrodes in the same layer; (b) with buried bus lines; (c) Photo of the fabricated LC lens; (d) The fabrication process for ring electrodes and buried bus lines.

#127370 - $15.00 USD Received 22 Apr 2010; revised 2 Aug 2010; accepted 3 Aug 2010; published 16 Aug 2010

With electrode widths determined, the optics of the designed LC lens is simulated to extract index distribution for estimating focusing power and quality. The simulation is carried out by using the commercial software DIMOS.2D to predict LC directors and then calculate index distribution via MATLAB for different drive voltages. Simulation was conducted in a 2D fashion and focused on a vertical cross section along the radius of the LC lens. The spatial resolution of the grid is 1000x101 for horizontal versus vertical. With LC reorientation solved, the effective refraction index distribution is computed column-wise based on Huygens principle [17]. This principle neglects the beam deviation in the LC layer. This a fair approximation since the ratio between the LC thickness and size is (50um/2mm) = 0.025. Figure 3 (a,b,c,d) shows simulated results of the refractive index distribution of GRIN lenses as opposed to the aperture radial position with 4, 6, 8 and 10 volts as the applied voltage on the outmost electrode ring (also the maximums), respectively. Table 1 lists the required simulated voltages applied to other inner electrodes. It is seen from these figures that the simulated index distribution follows closely to the desired one leading to a perfect GRIN lens, except for the central region where unsmoothnesses appear. These unsmoothnesses are caused by the large central electrode designed to cope with the relatively flat index gradient in the central region between r_9 and r_{10}, as shown in Fig. 2(c). The unsmoothnesses become more severe as the applied outmost voltage increases to achieve larger focusing power. However, in practice the index distributions in the central regions are expected smoother than those simulated by DIMOS due to the possible cross couplings between different columns of liquid crystals.

Table 2. Fabrication Parameters

Layer	Processing	Thickness
Glass substrate	-	550um
ITO	Sputtering	200nm
SU-8	Minus-photoresistance Coating > Soft-baking: step1. 65°C/1min; step2. 95°C/5min > Exposing > Developing > Hard-baking: 150°C/30min	1um ± 200nm
PI	Coating: 3000rpm/30s > Hard-baking: 200 deg C> Rubbing: 1.5 deg C	~1um before rubbing
LC	-	50um

3. Fabrication

The structure and fabrication process of the ring electrodes on a glass substrate for the proposed LC lens are stated in the followings. Based on the previous design, eight ITO transparent electrodes in ring type as marked in pinks in Fig. 4(a,b) are considered in the current study to validate the proposed LC lens design. Figure 4(a) depicts the baseline design where extensions of electrodes (e.g. bus lines) across rings are present, in order to apply varied voltages to inner/outer electrodes. This baseline design is implemented by the structure as shown in Fig. 2(b), where two glass substrates in thickness of 0.55 mm and coated with patterned 450Å-thick ITO ring electrodes are expected to be combined with a gap filled with liquid crystals. The ITO electrode owns, based on measurement, a transmittance of 94%. On the tops of the two patterned ITO glass substrates, polyimide (PI) layers (AL-1426B, from Daily-Polymer Corp.) are spin-coated for insulation and implementing rubbing. This spin-coating conducted at 3000 rpm for 30 seconds. After the spin-coating, the PI layer is baked at 200C for one hour. Table 2 shows the remaining fabrication parameters. Both PI layers are rubbed to form the micro-grooved surfaces, leading to LC pre-tilts of 2°. The two glass substrates are then stacked with 50um Mylar spacer in between. The LC E7 from Merck is filled in the gap between the two glass substrates. In addition, a layer of SU-8 of approximate 1 um is coated between the polyimide and ITO to render, as stated previously, smoother electrical field gradients. The details of the related fabrication steps are given in Table 2. Note that SU-8 is typically an excellent chemical negative resistance. Besides, SU-8 has high optical transmission above about 360 nm, degradation at 380°, and average adhesion to glass. Therefore, it is suitable herein to be coated between glass, ITO and PI. On the other hand, E7

#127370 - $15.00 USD Received 22 Apr 2010; revised 2 Aug 2010; accepted 3 Aug 2010; published 16 Aug 2010

adopted herein owns the ordinary refractive index, *no*, of 1.5183 and the extraordinary refractive index, *ne*, 1.7371. The elastic constants *K11*, *K22* and *K33* are 1.1, 5.9 and 17.1 pN, respectively. The dielectric constants, $\varepsilon_{//}$ and $\varepsilon_{\perp}$, are 19.28 and 5.21, along parallel and perpendicular directions, respectively. Finally, the rational viscosity is 233 m-Pa.

The eight ring electrodes in the afore-designed LC GRIN lens structure are, as shown in Fig. 2(b), in the same ITO layer. It is inevitable to extend the electrodes to cross rings to form bus lines for applying external voltages, as shown in Fig. 4(a). Theses bus lines (crossing extensions of electrodes) would definitely cause undesired electric fields in its local area and then result in unexpected LC rotations, eventually seriously undermining the imaging quality of the LC GRIN lens in this area. In addition to the afore-mentioned problem, it is also reported from [21] that the space between adjacent electrode rings ought to be large enough to avoid possible effects of short cuts. To remedy the above-problems, a new structure and associated fabrication process are proposed in this study, as illustrated by Fig. 4(b) and (d), respectively. Figure 4(c) show the photo of the fabricated LC lens. In this lens, the odd- and even-numbered electrodes are deposited and patterned at two different layers and separated by an insulator SU-8. In this way, as those red dots depicted in Fig. 4(b), the bus lines are buried below the layer of ring electrodes.

The details for fabricating different layers of electrodes are illustrated by Fig. 4(d) and stated in the followings. First, from (1) to (2), the ITO layer is patterned for the bus lines of all electrodes. These electrode bus lines are in radial extension to the outmost region of the glass substrate to be wire bounded. They do not cross each other in this layer. From (3) to (7), odd-numbered electrodes are formed with the ITO VIA holes connected the foundation and capsulated by insulating SU-8. Step (8) exposes the electrode pad for wire bounding. Steps (9) to (11) are for even-numbered ring electrodes. Also, Step (12) exposes the electrode pads for even-numbered rings to be wire bounded. By this design, the bus lines are buried below the conducting electrode rings such that the ring electrodes without crossing bus lines as shown in Fig. 4(b) can be realized. The distortions of electric fields in the local area around the bus lines as shown in Fig. 4(a) are avoided. Another advantage is that the neighboring electrodes need no spacing and the upper even-numbered electrodes could even be a little wider than originally designed in order to avoid over-etching in the process and also control the resistance to a lower value for a fast response. Figure 3(c) shows a photo of the fabricated GRIN LC lens following the afore-mentioned design and fabrication principles.

4. Experiment

With the designed GRIN LC lens fabricated, experiments are conducted next to validate the expected performance. Figure 5(a) illustrates the experiment setup for observing the focusing quality of the fabricated GRIN LC lens, as shown in Fig. 4(c). A He-Ne laser of wavelength 632.8nm is utilized as the light source. The emitted light beam passes through a 20X beam expander, an iris, a polarizer, the GRIN LC lens in radius 2mm, an analyzer and finally reaches a charge-coupled device (CCD). The iris is used for trimming the incident light from the laser to observe the interference pattern easily. The polarizing direction of the polarizer, rubbing direction of the PI films and that of the analyzer are in 45 degree difference subsequently, in order to generate desired circular interference patterns. Finally, for a clear interference pattern in the CCD the LC lens is placed at the focal point of the lens module of the CCD.

#127370 - $15.00 USD Received 22 Apr 2010; revised 2 Aug 2010; accepted 3 Aug 2010; published 16 Aug 2010

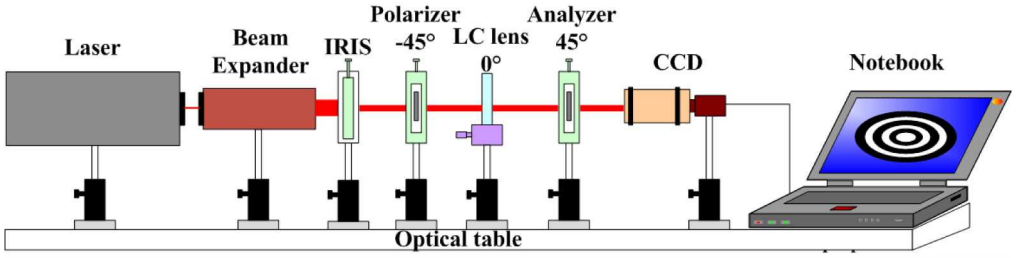

(a)

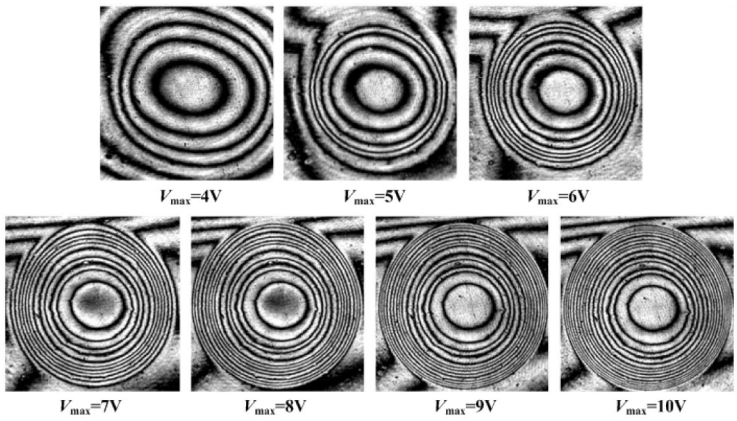

(b)

Fig. 5. (a) Experiment apparatus; (b) Interference patterns with the LC aperture in 2mm and the maximum applied driving voltages (to the outmost ring electrode) from 4V to 10V.

The measured interference ring patterns as shown in Fig. 5(b) represent the phase retardations of the LC GRIN lens [24]. Seven different sets of applied electrode voltages as are pre-calculated by DIMOS for application, as given by simulations in Table 1. It should be noted herein that reported from [9], LC disclination lines in a certain lens area easily occur due to the fixed pre-tilt angles of LCs near the PI alignment layers (2°) and the generated spatially non-uniform electrical field. To remedy the problem, prior to applying distinct top electrode voltages, a uniform electrical field is first applied between the top electrodes and the single bottom electrode. In this way, the disclination lines are eliminated. On the other hand, it is clearly seen from Fig. 5(b) that the interference rings are more densely present as the applied voltage increases, rendering shorter focus lengths of the LC GRIN lens. It should be also noted from this figure that the smooth circular interference patterns show no effects of electrical field distortions caused by buried bus lines. It is pertinent to mention herein that as reported in [25,26] the difference between the spherical geometry of the electrical field and the linear orientation of the LC director may cause a deformed interference pattern – an elliptic-like pattern. However, since the ratio of the aperture size to the LC thickness to is as large as (2mm/50um) = 40, the deformation of the interference pattern is negligible.

Deciphering the phase retardation patterns in Fig. 5(b), one is able to depict the resulted distributions of refractive index offered by this lens, as shown in Fig. 6(a), where the crosses represent the index distribution estimated from measured retardations. As seen from this figure, the closeness of the predicted indices to the measured data validates the effectiveness of the previous simulations and the satisfactory focusing quality offered by the fabricated LC lens. Furthermore, fitting the measured index distribution in Fig. 6(a) into a quadratic curve in Eq. (1), the focus length can be estimated. The estimated focal lengths are shown in Fig. 6(b), as opposed to varied levels of the maximum (for the outmost ring electrode) applied ring

#127370 - $15.00 USD Received 22 Apr 2010; revised 2 Aug 2010; accepted 3 Aug 2010; published 16 Aug 2010

voltage in 1kHz. Other than using the method of curve-fitting, in fact, based on the ring number of the interference pattern, *N*, one could also obtain the focal length by [27]

$$f = \frac{r^2}{2\lambda N}, \tag{5}$$

where *r* is the radius of the hole electrode and λ denotes the wavelength of the incident laser. It is seen from this subfigure that the achievable focus length is continuously shortened to 182.8 mm until the maximum applied voltage in 1kHz reaches the level around 10 volts, a relatively low driving voltage as compared to the most-common hole-type LC lenses [1]. To assess focusing quality, the average RMSE values between the measurements and fitted data for given focus lengths are calculated, and listed in Table 1 in terms of nominal visible wavelength of λ = 600 nm. A decrease in RMSE is seen as the focus length increases. Also, for the case with 10V drive on the outmost electrode, the average RMSE is 0.58λ. Although this number is still an order greater than 0.07λ, the common standard of focusing quality for a conventional solid lens, but still presenting some level of focusing effect. Further effort will be dedicated in the future to reach better quality and presented the next publication.

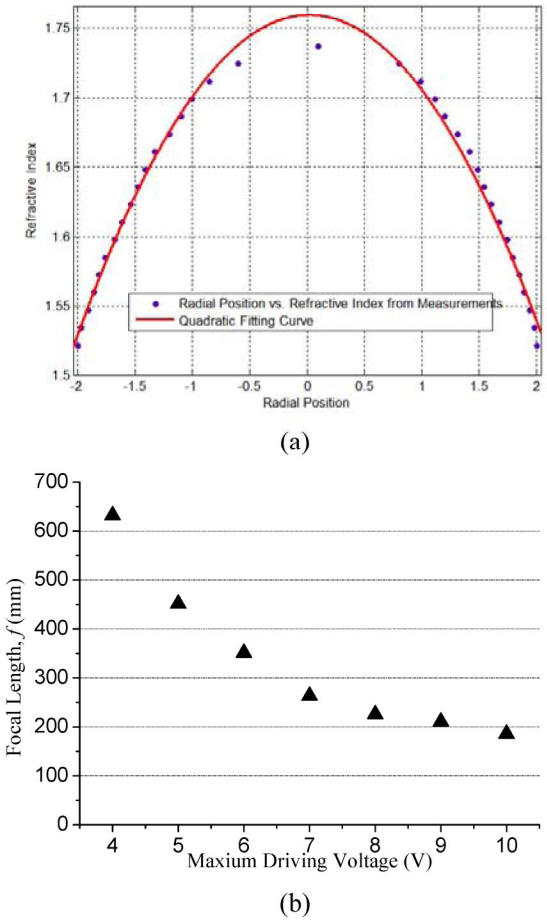

Fig. 6. (a) Measured and predicted index distributions with 10V applied to the outmost ring electrode; (b) Resulted focal lengths versus maximum (for the outmost ring electrode) driving voltages.

#127370 - $15.00 USD Received 22 Apr 2010; revised 2 Aug 2010; accepted 3 Aug 2010; published 16 Aug 2010

To observe the power distribution after the laser beam passes through the proposed lens, a beam analyzer, Ophir FX-50, is placed right after the analyzer (a CMOS sensor) instead of CCD camera. Setting the observing plane of the beam analyzer at its focal length, the power intensity distribution could then be analyzed. The intensity distributions of the fabricated LC GRIN lens, as shown in Fig. 4(c), with the outmost (maximum) ring voltages of 9V and 7V at 1 kHz are measured and presented in Fig. 7 in the forms of normalized point spread functions (PSFs). It is clearly seen from this figure that the distribution with a lower voltage, 7V, exerts lower peak intensity and wider sidebands, as opposed to 9V. This indicates that a higher driving voltage does render better focusing power. In addition, the diffraction spot size for the case with 9V (EFL in 210,7 mm) is about 0.15mm, 0.115 mm greater than the theoretical spot size of 0.035 mm. This shows that the focusing performance of the deigned LC lens is not up to but approaches the focusing quality of a conventional solid lens with tunability offered by the multiple ring electrodes.

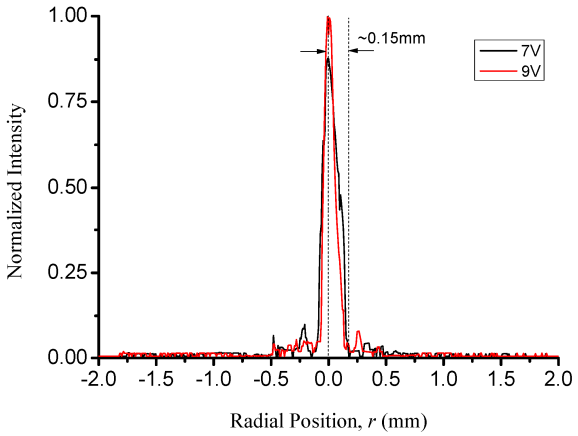

Fig. 7. Power intensity at the focal plane.

With quantitative measurements presented, the fabricated sample of the LC GRIN lens is installed in a camera module for a direct assessment in imaging quality. The measurement setup is illustrated by Fig. 8(a), where a polarizer with direction parallel to the rubbing direction of the LC lens is placed between the target object and the lens. Furthermore, a CMOS sensor array is used for recording images. For the assessment, the objective is moved from a relative far position to the lens, with the aim to check if the LC lens can adjust its EFL to obtain a clear image. The target image is placed 10 cm away from the CMOS sensor. The two photos in Fig. 8(b) and (c) show, respectively, the images taken by the CMOS sensor array before and after appropriate voltages are applied to eight electrode rings for focusing. A much clearer picture by subFig. 8(c) than 8(b) demonstrates favorable focusing capability of the proposed LC GRIN lens.

#127370 - $15.00 USD Received 22 Apr 2010; revised 2 Aug 2010; accepted 3 Aug 2010; published 16 Aug 2010

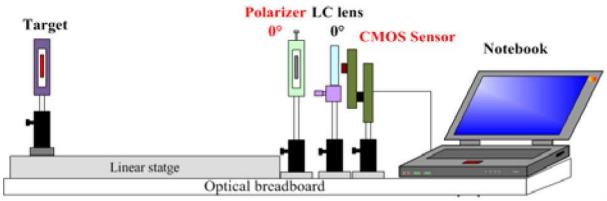

(a)

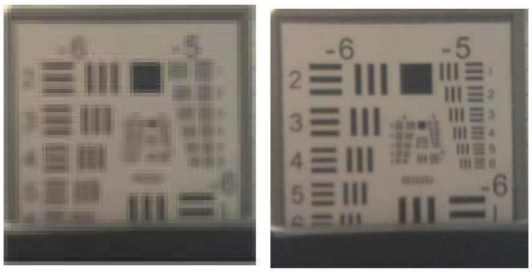

(b) (c)

Fig. 8. (a) The equipments of the image observation with a CMOS sensor; Images of the near object shot by a CMOS sensor with this proposed LC lens (b) not activated and (c) activated.

5. Conclusion

An LC lens with multiple ring electrodes in unequal widths is proposed in this work. This could be utilized in an AF and/or zooming system in cell cameras with satisfactory imaging quality in the future, in order to minimize its overall physical size. Placing the driving electrodes at the inner surface to the LC layer, the proposed LC lens is proven effective in reducing driving voltage level and yields a better refractive index distribution than the conventional LC lens with a hole-patterned electrode. A maximum applied voltage of 10V to the outmost ring electrode is able to achieve the focal length of 180 mm. To realize multiple electrodes, a new fabrication process for the multi-layer structure of an LC GRIN lens is proposed. The odd- and even-numbered electrode rings of the lens are placed in different layers, and bus lines are buried under these electrodes for avoiding distortions of the generated electric fields in imaging aperture. The measured interference patterns show favorable performances of the designed LC GRIN lens in maximizing focusing power, smoothing interference patterns and photo-imaging.

Acknowledgments

The authors are deeply indebted to the National Science Council, Taiwan, under the contracts NSC 98-2220-E-009-018 and 97-2221-E-009-057-MY3, for their financial support.

#127370 - $15.00 USD Received 22 Apr 2010; revised 2 Aug 2010; accepted 3 Aug 2010; published 16 Aug 2010